

## ARIPIPRAZOLE NANOSPONGE: NASAL IN-SITU GEL FORMULATION FOR NOSE TO BRAIN DELIVERY

Rana Zainuddin Ahmed<sup>1\*</sup>, Sonal Shaharwale<sup>2</sup>, Jaiprakash Sangshetti<sup>3</sup> and Shaikh Wasim Abdul Gani<sup>4</sup>

<sup>1,2,3</sup>Y.B. Chavan College of Pharmacy, Dr. Rafiq Zakaria Campus, Aurangabad- 431001, India.

<sup>4</sup>Shram Sadhana Bombay Trust's Institute of Pharmacy, Bambhori, Jalgaon- 425001, India.

Article Received on  
11 July 2022,

Revised on 01 August 2022,  
Accepted on 21 August 2022

DOI: 10.20959/wjpr202212-25396

### \*Corresponding Author

Dr. Rana Zainuddin  
Ahmed

Y.B. Chavan College of  
Pharmacy, Dr. Rafiq Zakaria  
Campus, Aurangabad-  
431001, India.

### ABSTRACT

Aripiprazole offers treatment for schizophrenia but the drug undergoes significant degradation in GI tract leading to poor bioavailability. The aim of present study is to formulate *in-situ* nasal gel for nose to brain delivery of Aripiprazole loaded nanosponge (ARP-NS) to achieve better treatment outcomes. **Method:** Nanosponges (NS) offer the advantage of enhanced dissolution, permeation and drug stability. NS were prepared using  $\beta$ -CD and diphenyl carbonate; parallel reaction synthesizer at temperature 85°C, 1000 rpm. The formulation was optimized for Carbopol 940 and HPMC K100 concentration using 3<sup>2</sup> factorial designs. The ARP-NS was characterized by FTIR, DSC, XRPD, zeta size and SEM. The formulations were evaluated for

parameters such as pH, drug content, viscosity, drug release, mucoadhesion, *ex-vivo* permeation and stability studies. **Results:** The PyMOL Molecular Graphics software was used to model  $\beta$ -CD NS and entrapment of Aripiprazole in the cavity, which along with other characterization techniques confirmed drug entrapment. Drug release from formulation and plain drug was found to be  $93.85 \pm 0.43\%$  and  $41.92 \pm 0.36\%$  respectively in 6 h. Treatment outcome was better from *in-situ* gel formulation compared to oral ARP solution on performing locomotor studies on psychosis induced rats. Pharmacokinetic evaluation was performed on Sprague dawley male rats. C<sub>max</sub>, T<sub>max</sub> & AUC of ARP-NS (in brain) was found to be  $4929 \pm 21.56$  ng/mL, 3 h and  $930.35 \pm 24.5$  ng.h/mL. **Conclusion:** This study showed that Aripiprazole could be delivered effectively to the brain using nanosponge incorporated in *in-situ* gel which produced sustained drug release.

**KEYWORDS:** Nanosponges, nose to brain delivery, Schizophrenia, Pharmacokinetics, locomotor activity.

## INTRODUCTION

Schizophrenia is a debilitating psychiatric disorder and can have a negative impact if untreated. Individuals with schizophrenia are at considerable psychosocial and biological risks associated with relapse. Aripiprazole is a drug of potential in monotherapy or combination therapy for patients with treatment-resistant schizophrenia.<sup>[1]</sup> Chemically Aripiprazole (ARP) is 7-[4-[4-(2, 3-dichlorophenyl)-1- piperazinyl] butoxy]-3, 4 dihydrocarbostyryl and has partial agonist activity at D2 and 5-HT1A receptors and antagonist activity at 5-HT2A receptors.<sup>[2,3]</sup> It was launched in 2002 for the treatment of schizophrenia in adults. Common gastrointestinal side effects include nausea, upset stomach and vomiting. The elderly also face a choking hazard while swallowing tablets. The drug is poorly soluble (0.00777mg/mL) and poorly permeable.<sup>[4]</sup> The mechanism postulated for antipsychotic action of ARP is through lowering dopaminergic neurotransmission in the mesolimbic pathway and enhancing dopaminergic activity in the mesocortical pathway.<sup>[5]</sup> Intra nasal drug delivery is a lucrative approach since drugs administered into the nasal cavity can be rapidly absorbed into systemic circulation without the usual enzymatic degradation and hepatic first-pass effect accompanying oral administration, resulting in enhanced bioavailability and rapid onset of the pharmacological effects.<sup>[6,7]</sup> The scientific fraternity is taking profound interest in nasal drug delivery as an alternate route for drug delivery; especially for those moieties susceptible to inactivation due to various metabolic processes and those unable to cross the blood brain barrier.<sup>[8,9]</sup> Nasal drug delivery has taken a step further to overcome limitation of nasal clearance by adopting *in-situ* gels.<sup>[10-12]</sup> Carbopol 940 derivatives are popularly used in mucoadhesive drug delivery systems for application to nasal mucosa. The most prominent advantage of *in-situ* gels over the conventional gel is that it can be conveniently and accurately instilled as a drop allowing patient-friendly, needle-free dosage form.<sup>[13]</sup> Marketed products of ARP include tablets, oral solution and IM injections. Research articles have reported study on long-acting injectables,<sup>[14]</sup> gummi formulation,<sup>[15]</sup> depot intra muscular injection, and ARP loaded nanoparticles.<sup>[16]</sup> Our approach involved the use of nanosponges which have gained immense popularity due to many inherent advantages. They are biocompatible and can enhance drug permeability.<sup>[17,18]</sup> Further, NS can be modulated to provide the desired drug release characteristics like pH and time dependent nano-carriers and

controlled release.<sup>[19-22]</sup> To our knowledge there are no reports of a nasal NS formulation. We prepared a nose to brain formulation of nanosponge for delivery of an anti-psychotic drug.

## MATERIAL AND METHODS

### Materials

ARP was obtained as gift sample from Cipla Pvt. Limited, Mumbai, India. Carbopol 940 was purchased from Loba chemicals, Mumbai, HPMC K100, Benzalkonium chloride was purchased from Merk Limited, Mumbai,  $\beta$ -cyclodextrin Himedia Laboratories Pvt. Ltd, diphenyl carbonate was purchased from Thermo Fisher Scientific India Pvt. Ltd, India, Acetonitrile HPLC grade was purchased from Spectrochem Pvt. Ltd, Mumbai and all other chemicals were procured in-house. HPLC [GraceSmart, C18 RP column, 250mm $\times$ 4.6mm, flow rate of 1ml/min].

### Methods

#### Preparation of $\beta$ -Cyclodextrin nanosponges

$\beta$ -CD: DPC in 1:4 stoichiometric ratio were added to 10 mL of DMF and heated at 85°C for 15 min at 900-1000 rpm in a parallel reaction synthesizer. Completion of the reaction was indicated by observing precipitation. The insoluble product was washed with excess water followed by ethanol. The obtained NS was dried overnight at 60°C and stored until further use.

#### Drug entrapment

Drug solution was prepared in acetonitrile and 1:4 CD-NS formulation was allowed to equilibrate with drug solution for 24 h on the rotary shaker. Amount of aripiprazole entrapped was determined by UV spectroscopic method (UV-Shimatzu 1800 double beam) at 255 nm.

#### Characterization studies

The IR spectrum of ARP-NS was obtained using KBr pellet technique using PS 4000 (Jasco Japan). The pellets were scanned over a range of 4000 to 400 cm<sup>-1</sup>. The FTIR spectrum was analysed for confirming formation of NS.<sup>[23]</sup>

The X-ray powder diffraction patterns of powdered sample of ARP-NS were determined by using Bruker AXS D8 Advance X-ray diffractometer. Sample was irradiated with monochromatized Cu K alpha radiation (1.5406Å) and analyzed between 3-70° (2 $\theta$ ). The voltage and current used was 40kV and 30mA respectively.

DSC thermograms of ARP and ARP-NS were obtained using differential scanning calorimeter (Shimadzu, Japan.) Flow rate of nitrogen was maintained at 100 mL/min and the heating rate was 10°C at the scanning rate of 10°C/min over a temperature range of 10°C to 300°C.

Particle size distribution and zeta potential determination were carried out in distilled water using zeta sizer Nano ZS (Malvern Instrument Ltd, UK). Particle size and zeta potential were measured.

Surface structure of NS was observed under a scanning electron microscope (EVO-18, Zeiss, Germany). The lyophilized sample was platinum coated, placed in aluminum stubs and viewed at different magnification in an accelerating voltage of 15.00 kV.

### Preparation and Optimization of mucoadhesive in-situ gel

Required amount of Carbopol 940 was weighed and transferred to a beaker containing 10mL of distilled water, the contents were stirred to break up lumps. It was heated up to 50°C for 15 to 20 min and kept aside to cool, in the second beaker required amount of HPMC K100 and 10mL of water was added and stirred using mechanical stirrer to form a clear solution. The contents of the first beaker were added to the second beaker containing HPMC K100 and stirred till formation of clear liquid and keep aside for cooling. Finally, ARP-NS and 0.1% solution of benzalkonium was added to the polymer solution. The formulation was then stored at room temperature in a suitable airtight container.

Nine gel formulations were prepared and optimized using Design expert software, 2017 based on  $3^2$  factorial design considering Carbopol 940 and HPMC K100 independent variables. The batches consisted of drug loaded NS equivalent to 50 mg, 0.1% of benzalkonium chloride and varying concentrations of Carbopol 940 and HPMC K100. The formulation design levels are given in table 1 & batches are presented in table 2.

**Table 1: Levels of batches.**

|                       | Levels |     |     |
|-----------------------|--------|-----|-----|
| Independent variables | -1     | 0   | +1  |
| Carbopol940           | 0.2    | 0.4 | 0.6 |
| HPMC K100             | 0.2    | 0.4 | 0.6 |

**Table 2: Formulation batches of ARP-NS.**

| Sr. no. | Code | Carbopol940<br>(%w/v) | HPMC K100<br>(%w/v) |
|---------|------|-----------------------|---------------------|
| 1       | F1   | 0.4                   | 0.6                 |
| 2       | F2   | 0.4                   | 0.2                 |
| 3       | F3   | 0.6                   | 0.6                 |
| 4       | F4   | 0.6                   | 0.4                 |
| 5       | F5   | 0.2                   | 0.4                 |
| 6       | F6   | 0.6                   | 0.2                 |
| 7       | F7   | 0.2                   | 0.6                 |
| 8       | F8   | 0.2                   | 0.2                 |
| 9       | F9   | 0.4                   | 0.4                 |

**Evaluation**

- Gel strength and Mucoadhesive strength**

The gel strength was determined by placing a weight of 35 g on 50 g sample of the nasa gel taken in a 100 mL graduated cylinder, the time required by the weight to penetrate 5cm into the gel was recorded.<sup>[24]</sup>

Mucoadhesive strength was determined using the modified method reported by Yong CS. A section of goat nasal mucosa was fixed on two glass slides using thread. A quantity of 50 mg of gel was placed on the first slide which was placed below the height adjusted pan. While another slide with mucosal section was fixed in inverted position on the underside of same pan. Both the slides, with gel formulation between them, were held in intimate contact between them for 2min. The mucoadhesive force, expressed as the detachment stress in dynes/cm<sup>2</sup>, was determined from the minimal weight that caused detachment of the mucosal tissue from the surface of formulation.<sup>[25]</sup>

- Drug content**

A 1mL sample of gel was taken in a 100 mL volumetric flask and diluted with phosphate buffer pH 5.5. The contents of the flask were shaken to ensure extraction of drug into the solvent. The solution was filtered through 0.2 µm filter paper and drug content was determined using a UV spectrophotometer at 255nm.

- pH and Viscosity measurement**

The pH of each formulation was determined by using pH meter. The viscosity measurements were carried out by using Brookfield programmable DV-III/V model. The gel sample was placed in small adapter. Viscosity at RT was recorded using suitable spindle.

- **In- vitro release Study and Ex- vivo permeation study**

Drug release from gel was tested on a cellophane membrane (mol.wt.12000-14000 Da) with permeation area  $0.45\text{cm}^2$  using Franz diffusion cell. A 20mL of pH 5.5 phosphate buffer was added to the acceptor chamber. Gel containing drug equivalent to 50mg was placed in donor compartment. At predetermined time points, 1mL sample was withdrawn from acceptor compartment over a period of 6h while replacing the aliquot to maintain sink conditions. The aliquots were suitably diluted with phosphate buffer and measured spectrophotometrically at 255nm to determine the concentration. The same setup was used for performing the *ex-vivo* permeation studies using goat nasal mucosal membrane.<sup>[26]</sup>

- **Stability studies**

Accelerated stability studies were performed according to ICH guidelines,  $40^\circ\text{C} \pm 2^\circ$ , 75% RH  $\pm 5$ . Amber coloured vials of gel samples were kept in the stability chamber. Samples were withdrawn at pre-determined intervals for 6 months and evaluated for drug content and pH.<sup>[27]</sup>

- **Statistical analysis**

All the data are reported as mean  $\pm$  standard deviation (SD). Differences between the groups were compared using ANOVA (analysis of variance). A p-value  $<0.05$  was considered as statistically significant which was calculated by graph pad instat software.

### **Pharmacokinetic studies**

Sprague Dawley male rats were used for *in-vivo* studies of the finalized batch for bioavailability assessment and effect on psychosis induced animals. The protocol for animal studies was approved by Institutional animal ethical committee (CPCSEA/IAEC/QA-7/2017-2018/131). Animals were made comfortable in plastic cages with paddy husk in a controlled environment.

The animals were divided into three groups as follows each group containing 3 animals.

Group I: 3 Animals-Normal control

Group II: 3 Animals-*In-situ* nasal gel (0.89 mg/kg)

Group III: 3 Animals-ARP oral solution (0.89 mg/kg)

Group IV: 3 Ketamine control

Group I rat (n=3) was orally given 0.9% saline solution and other groups were treated with ARP-NS *in-situ* nasal gel and oral solution respectively. Group II rats were administered 0.1mL of *in-situ* gel in one nostril using a micropipette. Group III rats were fed ARP oral solution by feeding tube. Animals were anaesthetized in CO<sub>2</sub> chamber and the capillary retro-orbital plexus was punctured to withdraw 0.2mL blood which was collected in EDTA coated eppendorf tubes over a 24 h period at pre-determined time intervals (0.25, 0.5, 1, 2, 4, 6, 8, 12 and 24 h). The collected blood samples were immediately centrifuged (Cooling centrifuge, Sigma instruments, Germany) at 4000 rpm for 10 min to segregate the plasma, 1 mL of diethyl ether was added to the obtained plasma sample and centrifuged at 4000 rpm for 10 min, to separate the organic layer which was evaporated to dryness at room temperature to obtain extracted ARP. The resulting extraction residue was reconstituted in acetonitrile-methanol-water-acetic acid (27:25:48:1, v/v/v/v) and aliquot was injected in HPLC system. Simultaneously, the animals were sacrificed by administration of overdose of pentobarbitone sodium and brain was removed and washed with normal saline. It was homogenized with normal saline solution by using homogenizer. The homogenate were centrifuged at 4000rpm for 20min (4°C), and aliquots of the supernatant were separated and stored at -20°C until drug analysis was carried out using HPLC.<sup>[28]</sup>

### Behavioural study

Group II, III and IV were injected with 50mg/kg ketamine solution for 3 days. Actophotometer was applied to confirm induction of psychosis. After 1 hour of dosing activity was recorded for 5 min.<sup>[29,30]</sup>

## RESULTS AND DISCUSSION

### *Characterization and Evaluation*

Drug entrapment efficiency was found to be 90%. FTIR spectrum of ARP showed the characteristic peaks of the drug. The spectrum of nanosponge was taken to confirm the formation of carbonate linkage between diphenyl carbonate and  $\beta$ -CD which was confirmed by characteristic peak at 1774 cm<sup>-1</sup> (Figure 1).



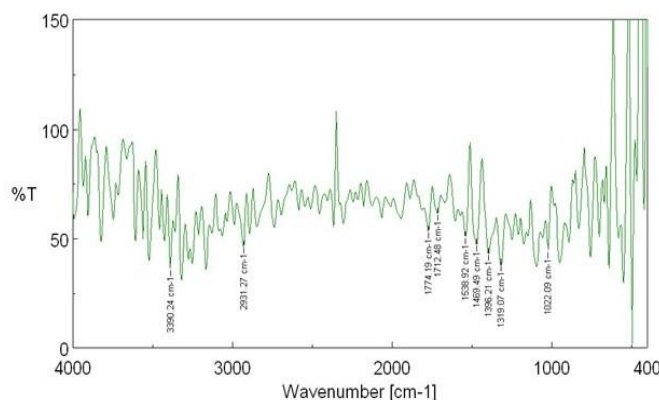


**Figure 1: Infrared spectra of nanosponge.**

DSC thermogram of ARP showed a sharp peak at 138.5°C due to crystalline nature of drug. Incorporation of drug within the NS cavity leads to decrease in drugs 'crystallinity' which was confirmed from the ARP-NS thermogram having reduced peak intensity, indicating encapsulation of drug (Figure 2).

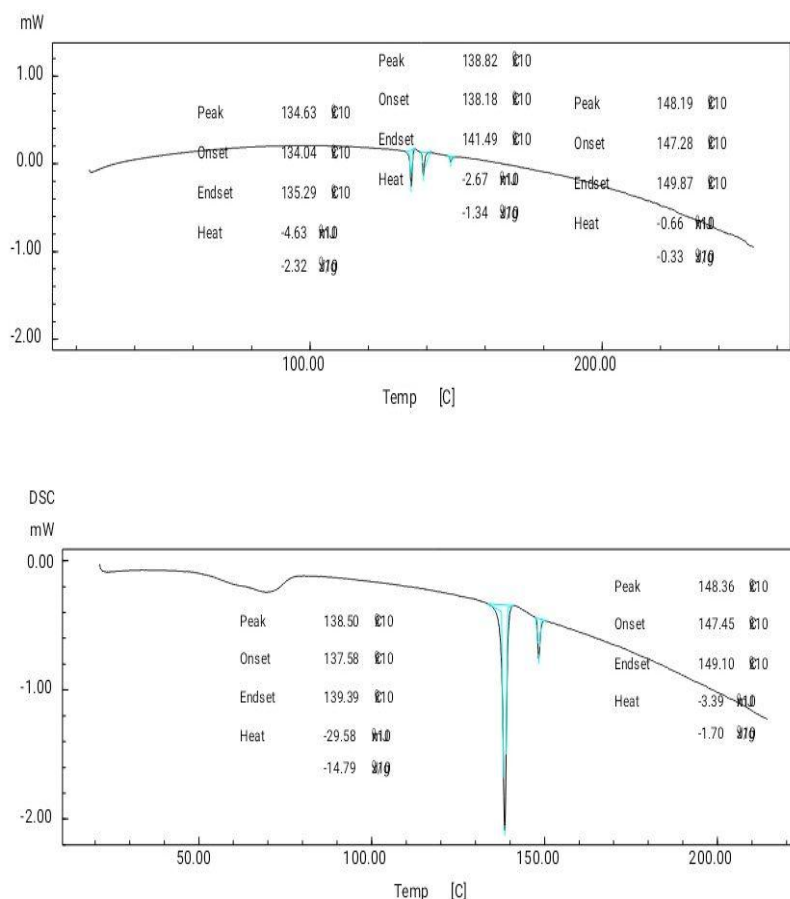


**Figure 2: DSC Thermogram of (a) ARP-NS and (b) ARP.**

X-ray diffraction was also used to confirm drug incorporation. The XRD pattern of ARP showed sharp peaks at  $2\theta$ -scattered angles at  $29.438^\circ$  and  $21.489^\circ$ , where as the peaks were



diffused on complexation, which confirms formation of amorphous form of ARP-NS and intercalation of ARP in host cavity of CD (Figure 3).

Figure 3: XRPD of (a) ARP-NS and (b) ARP.

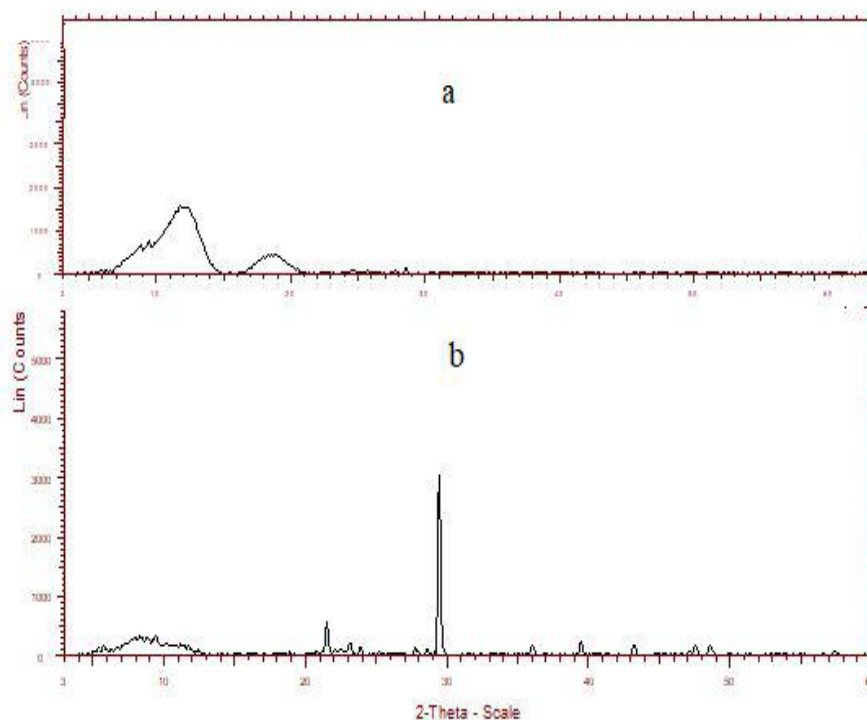


Figure 3: XRPD of (a) ARP-NS and (b) ARP.

Scanning electron microscopy of CD-NS shows a porous topography due to presence of nano-cavities. In zeta sizer analysis PDI was found to be 0.763. Zeta potential for average particle of 71.6nm was found to be 3.22 mV.

### Drug Content and pH

The drug content of all the prepared gel formulations was checked and found to be in the range of  $94.5 \pm 0.11$  to  $95 \pm 0.19\%$ . Normal physiological pH of the nasal mucosa is 4.5–6.5; the nasal mucosa can tolerate solutions within a pH range of 3-10. The pH of all the formulations (F1 to F9) was found to be within  $5.9 \pm 0.13$  to  $6 \pm 0.18$ , which was between physiological ranges of pH of nasal mucosa.

### Mucoadhesive strength

All the formulations were subjected to mucoadhesion study. The mucoadhesion force is an important parameter for *in-situ* gelling nasal formulations; it prolongs residence time in the

nasal cavity. The bioadhesive force generally depends on the nature and concentration of the bioadhesive polymers. The stronger the bioadhesive force, longer is the nasal residence time. All formulation (F1 to F9) shows mucoadhesive strength between 1592.5 to 2817.5 dyne/cm<sup>2</sup> (Table 3, Figure 4).

**Table 3: Evaluation parameter of batches F1 to F9 (Mean  $\pm$  SD, n=3).**

| Formulation Code | Mucoadhesive Strength (dyne/cm <sup>2</sup> ) | Gel strength (sec) | Viscosity          | % Drug release in 6h |
|------------------|---|--------------------|--------------------|----------------------|
| F1               | 2327.5 $\pm$ 1.23                             | 21 $\pm$ 0.23      | 1329.7 $\pm$ 0.46  | 91.69 $\pm$ 0.65     |
| F2               | 2082.5 $\pm$ 0.41                             | 12 $\pm$ 0.48      | 1192.45 $\pm$ 1.39 | 79.78 $\pm$ 0.47     |
| F3               | 2817.5 $\pm$ 0.68                             | 13 $\pm$ 0.13      | 1819.21 $\pm$ 0.64 | 58.35 $\pm$ 0.11     |
| F4               | 2695 $\pm$ 0.76                               | 16 $\pm$ 0.19      | 1619.92 $\pm$ 0.72 | 73.52 $\pm$ 0.24     |
| F5               | 1837.5 $\pm$ 0.94                             | 20 $\pm$ 0.72      | 983.6 $\pm$ 0.63   | 84.46 $\pm$ 0.12     |
| F6               | 2450 $\pm$ 0.87                               | 19 $\pm$ 0.34      | 1516.74 $\pm$ 0.17 | 70.03 $\pm$ 0.35     |
| F7               | 1960 $\pm$ 0.36                               | 32 $\pm$ 0.89      | 1009.4 $\pm$ 1.36  | 93.85 $\pm$ 0.43     |
| F8               | 1592.5 $\pm$ 1.64                             | 25 $\pm$ 0.14      | 824.6 $\pm$ 0.43   | 82.46 $\pm$ 0.62     |
| F9               | 2205 $\pm$ 1.29                               | 29 $\pm$ 0.64      | 1264.5 $\pm$ 1.24  | 75.52 $\pm$ 0.17     |

Design-Expert® Software  
Trial Version  
Factor Coding: Actual

mucoadhesive strength (dyne/cm<sup>2</sup>)

● Design points above predicted value

○ Design points below predicted value

1592.5 2817.5

X1 = A: carbopol940

X2 = B: HPMC K100

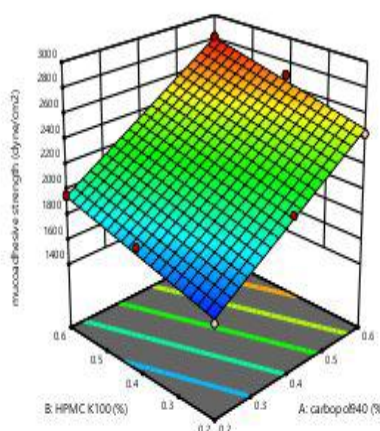


**Figure 4: 3-D graph showing effect of excipients on mucoadhesive strength.**

### Mathematical model fitting

Batch F7 (n=3) showed the highest percentage of drug release that is 93.85 %  $\pm$  0.43 in 6h min and all batches showed probability <0.05, which is statistically significant calculated by Graph pad instat software.

Model fitting will provide the understanding about the release mechanism. The kinetics of drug release was determined by fitting the best fit of the dissolution data to distinct models.

According to the correlation coefficient values ( $r^2$ ), the drug release from the nanosponge loaded gel could be described by first order kinetics, HPMC K 100 was used as a hydrophilic release retardant polymer. The results obtained from release rate of the drug from the gel are highly influenced by the concentration of HPMC.

For insoluble drug incorporated in a porous matrix, the amount of drug released is proportional to the amount of drug remaining in the matrix. Thus, the amount of active released tends to decrease as a function of time. Since  $n$  was less than 0.5, therefore it follows fickian diffusion with first-order release. Swelling of the matrix is responsible for this type of behaviour.

Carbomer is a cross-linked polymer, and the large number of carboxyl groups contributed to fast swelling of the polymer matrix due to electrostatic repulsion forces between negatively charged segments of the polymer. Pronounced swelling and the cross-linked structure of the carbomer contributed to the formation of a stable mechanic mucoadhesive bond that could be further stabilised by hydrogen bonds. The amorphous inclusion complex in the polymer matrix could promote hydration of the matrix, acting as a channelling or wicking agent. Thus, the polymer matrix containing HPMC and carbopol could swell and also enhance mucoadhesion. The F7 batch was selected as the optimized formulation. Highest extent of drug release was observed at the lowest levels of carbopol and high level of HPMC giving a rate controlling effect. Comprehensive analysis of surface response plots depicted the need of establishing a balance between the two polymers in order to obtain sufficient mucoadhesiveness to the nasal mucosa while providing sustained and complete drug release from the gel. Around 60% of drug was released within an hour, after which the release was sustained upto 6 h (Figure 5 and 6).

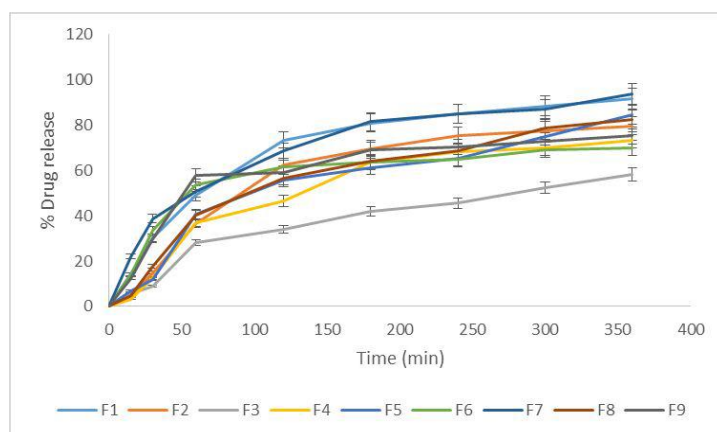


Figure 5: % Drug release of formulation (F1 to F9 batches).

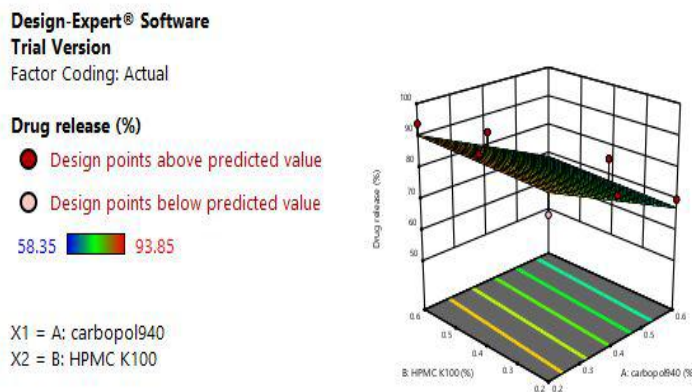


Figure 6: 3-D graph showing of excipients on drug release.

### Ex-vivo permeation study

The drug permeation from the NS incorporated gel gave better results in terms of higher rate with a two-fold increase in permeation within half an hour followed by a steady rate. The presence of nanosponge in the gel formulation enhanced the drug permeation when compared to drug gel. The mucoadhesive properties of polymer ensured that the gel was in favourable contact with the nasal mucosa ensuring good drug permeation of  $89.23 \pm 0.34$  in 6 h (Figure 7).

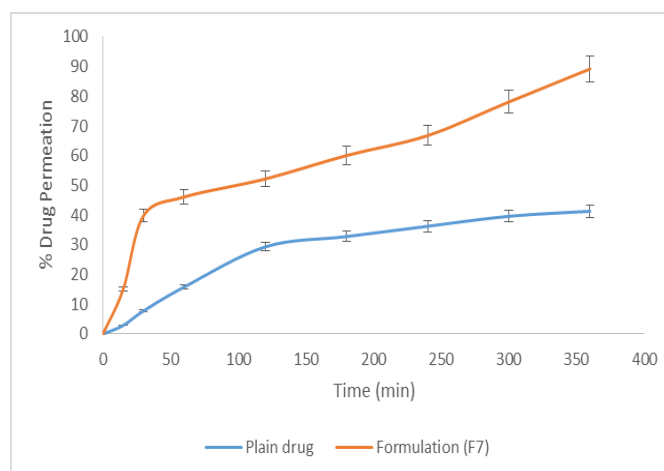


Figure 7: *Ex-vivo* permeation of plain ARP Solution and ARP-NS gel ( $p < 0.05$ ).

### Molecular modelling studies

The PyMOL Molecular Graphics System and Discovery studio 4.1 software was used to model  $\beta$ -CD NS and entrapment of Aripiprazole in the cavity. The 3D structures of Aripiprazole,  $\beta$ -CD & hypothetical NS were drawn and optimized using the Discovery studio 4.1. Aripiprazole was manually docked into the  $\beta$ -CD NS cavities. The analysis of

entrapment was done on the basis of Vander Waals surface, solvent accessible surface and hydrophobic regions in the  $\beta$ -CD NS cavity.

The structure of Aripiprazole consists of middle butyloxy chain and two bulkier substituent i.e. 1, 2, 3, 4-tetrahydroquinoline-2-one and 2, 3-dichlorophenyl substituted piperazine ring. The  $\beta$ -CD cavity has a hydrophobic interior of diameter 8-8.5 Å and width 5-6 Å. The hydroxyl groups of  $\beta$ -CD are trans esterified with carbonate spacer groups resulting in formation of polymeric  $\beta$ -CD nanosponge. The structural investigations of optimized structure of Aripiprazole showed the length of butyloxy chain as 7.4 Å, whereas the distance between two extremely placed atoms is 11.7 Å. This optimized structure could be entrapped in  $\beta$ -CD cavity such that the hydrophobic butyloxy chain is well placed in hydrophobic interior of  $\beta$ -CD cavity of width 5-6 Å. The top and bottom rim of  $\beta$ -CD is hydrophilic due to hydroxyl groups. In this hydrophilic area of  $\beta$ -CD two bulkier groups of Aripiprazole can occupy. Such placement of Aripiprazole is favoured due to presence of hydrophilic oxygen of butyloxy and nitrogen of piperazine. Figure 8 depicts the hypothetical entrapment of Aripiprazole in the nanosponge cavity.

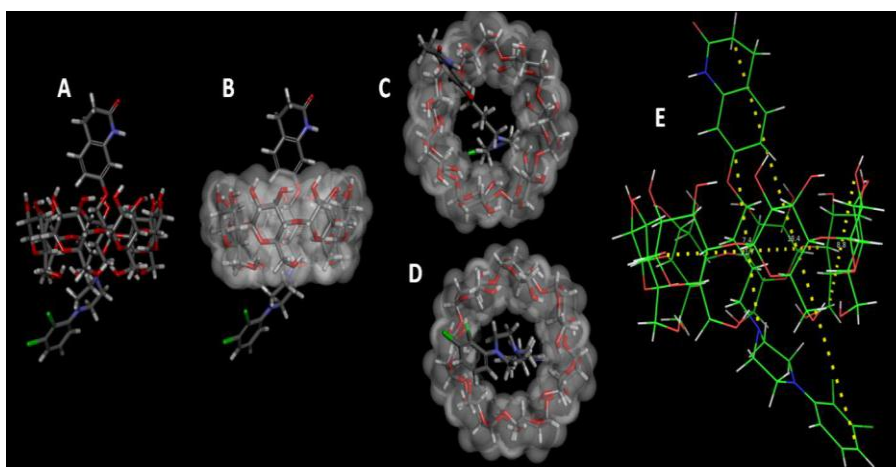


**Figure 8: Entrapment of Aripiprazole in the  $\beta$ -CD cavity. A) Side view, B) Solvent accessible surface around  $\beta$ -CD cavity, C) Top view, D) Bottom view, E) Measurement of distance.**

### Animal behaviour study

The locomotor activity was evaluated to compare the antipsychotic effects of optimized nasal formulation. The locomotor activity was observed post 3 hours of dose administration. The results were compiled based on number of times the rats crossed the lines in 5 min. The normal control group animals crossed  $237.86 \pm 4.96$ , ketamine control  $51.53 \pm 1.05$ ,

ketamine + oral ARP  $84.06 \pm 3.03$  and ketamine + nasal formulation  $203.93 \pm 93$  times. Where,  $n=3$ , (mean  $\pm$  SD), analysed by ANOVA method and  $p < 0.05$  when compared with ketamine control group,  $p < 0.05$  compared with normal group,  $p < 0.05$  compared with oral ARP and is  $p < 0.05$  compared with nasal formulation. Improved locomotor activity was observed when ARP was administered as a nanosponge through in-situ nasal gel.

### Pharmacokinetic study

The pharmacokinetic parameters of drug after intranasal and oral administration were investigated. The ARP given by the oral route shows the  $C_{max}$ ,  $T_{max}$  and AUC in brain are lesser than nasal route. The concentration of drug in the brain was found to be increased when given through nasal route as compared to the oral route. The probability of the formulation after oral and intranasal was  $< 0.05$ , which was significant. Kinetica 5.0 software was applied for pharmacokinetic parameters calculation (Data shown in Table 4, Figure 9 & 10).

**Table 4: Pharmacokinetic parameter of ARP after nasal and oral administration to rats in Brain and Plasma. (Mean  $\pm$  SD,  $n=3$ ;  $p < 0.05$ )**

| Parameter         | Nasal             |                   | Oral              |                  |
|-------------------|-------------------|-------------------|-------------------|------------------|
|                   | Brain             | Plasma            | Brain             | Plasma           |
| $C_{max}$ (ng/ml) | $4929 \pm 21.56$  | $1986 \pm 24.23$  | $3152 \pm 18.21$  | $4395 \pm 29.47$ |
| $T_{max}$ (h)     | 3                 | 2                 | 4                 | 3                |
| AUC (ng.h/ml)     | $930.35 \pm 24.5$ | $479.46 \pm 12.4$ | $319.72 \pm 16.5$ | $433.09 \pm 9.4$ |

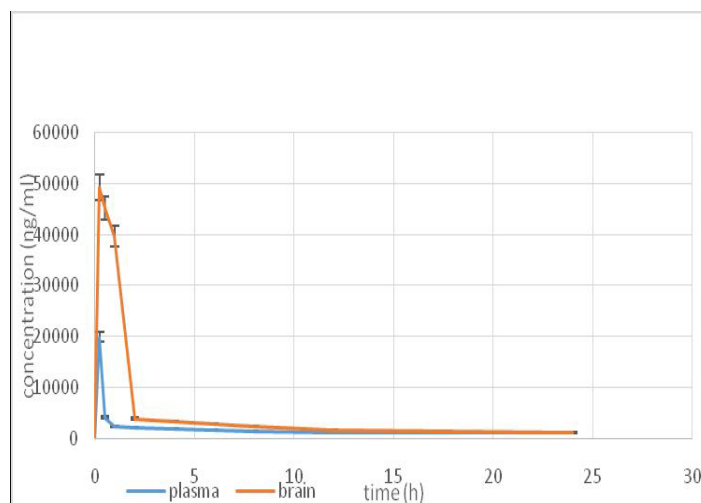


**Figure 9: Drug concentration versus time profile of ARP-NS in the Plasma and Brain after nasal administration ( $p < 0.05$ ).**



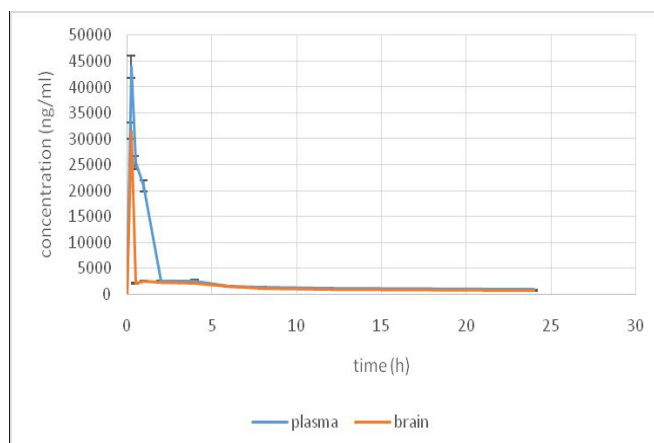


**Figure 10: Drug concentration versus time profile of ARP-NS in the Plasma and Brain after oral administration ( $p < 0.05$ ).**

### 3<sup>2</sup> Factorial design

Carbopol 940 and HPMC K100 were two independent variables were selected and their effects on the responses (drug release and mucoadhesive strength) were studied by using design expert software version 11 (Table 5).

**Table 5: 3<sup>2</sup> factorial design.**

| Std | Run | Factor 1<br>A: Carbopol<br>940 (%) | Factor 2<br>B: HPMC<br>K 100 (%) | Response 1<br>Mucoadhesive<br>strength (dyne/cm <sup>2</sup> ) | Response 2<br>Drug release<br>(%) |
|-----|-----|------------------------------------|----------------------------------|--|-----------------------------------|
| 3   | 1   | 0.4                                | 0.6                              | 2327.5   | 91.69                             |
| 2   | 2   | 0.4                                | 0.2                              | 2082.5   | 79.48                             |
| 1   | 3   | 0.6                                | 0.6                              | 2817.5   | 58.35                             |
| 4   | 4   | 0.6                                | 0.4                              | 2695   | 73.52                             |
| 9   | 5   | 0.2                                | 0.4                              | 1837.5   | 84.46                             |
| 7   | 6   | 0.6                                | 0.2                              | 2450   | 70.03                             |
| 6   | 7   | 0.2                                | 0.6                              | 1960   | 93.85                             |
| 8   | 8   | 0.2                                | 0.2                              | 1592.5   | 82.46                             |
| 5   | 9   | 0.4                                | 0.4                              | 2205   | 75.52                             |

### CONCLUSION

Drug delivery of drugs acting on CNS is always challenging, however, nose to brain delivery can overcome such limitations. The use of nanosponges for this route of administration has not been studied till now. NS offer varied applications such as enhancing drug dissolution, stabilizing the entrapped moieties and release the drug at the targeted site of action.  $\beta$  cyclodextrin nanosponges were synthesized and characterized. The application of PyMOL Molecular Graphics System and Discovery studio 4.1 software confirmed the possibility of drug entrapment in to the  $\beta$  -CD NS cavity. Aripiprazole was loaded into the NS and an



optimized *in-situ* nasal gel was formulated using a  $3^2$  factorial design. Optimized concentration of Carbopol940 and HPMC K100 gave required integrity to the gel at nasal pH and sustained the drug release. The pharmacokinetic parameters were measured on the rats. ARP-NS delivery through nasal route was more rapid and effective to the brain compared to the oral route. Increase in Cmax and simultaneous drop Tmax led to faster on- set. Behavioural studies concluded that the nasal formulation was more effective compared to oral ARP administration and showed improvement in locomotor activity. Oral formulations generally have multiple side effects and first pass metabolism decreases efficacy. Hence, as supported through this study, delivering ARP formulation through nasal route increased drug concentration in brain and improved the locomotor activity in psychosis induced rats.

### Abbreviations

ARP-NS: Aripiprazole loaded nanosponge; GI tract: Gastro intestinal tract; NS: Nanosponges  
HPMC: Hydroxypropyl methylcellulose;  $\beta$ -CD:  $\beta$ -Cyclodextrin; FTIR: Fourier transform infrared spectroscopy; DSC: Differential scanning calorimetry; XRPD: X-ray powder diffraction; SEM: Scanning electron microscope; KBr: Potassium Bromide.

### Acknowledgement

The authors are thankful to Mrs. Fatma Rafiq Zakaria, Chairman, Maulana Azad Educational Trust, Aurangabad 431001(M.S), India, for her continuous motivation and support. The authors are deeply thankful to Dr. Ayaz Ali, Associate Professor, Y.B Chavan College of Pharmacy, Aurangabad (India) for his assistance in performing pharmacokinetic and biodistribution studies.

### Conflict of interest

The authors declare that there is no conflict of interest.

### REFERENCES

1. Mossaheb N and Kaufmann RM. Role of aripiprazole in treatment-resistant schizophrenia Neuropsychiatr. Dis. Treat, 2012; 8: 235–244. doi: 10.2147/NDT.S13830.
2. Sawant K, Pandey A, Patel S. Aripiprazole loaded poly (caprolactone) nanoparticles: Optimization and in vivo pharmacokinetics. Mater Sci Eng C Mater Biol Appl, 2016; 66: 230-243. doi: 10.1016/j.msec.2016.04.089.

3. Bortolozzi A, Díaz-Mataix, L, Toth M, Celada P, Artigas F. In vivo actions of aripiprazole on serotonergic and dopaminergic systems in rodent brain. *Psychopharmacology*, 2007; 191: 745–758. doi:10.1007/s00213-007-0698-y.
4. <https://pubchem.ncbi.nlm.nih.gov/compound/Aripiprazole#section=3D-Conformer>.
5. Mei H, Xu-Feng H, Chao D. Aripiprazole differentially affects mesolimbic and nigrostriatal dopaminergic transmission: implications for long-term drug efficacy and low extrapyramidal side-effects. *Int J Neuropsychopharmacol*, 2009; 12(7): 941–952. doi: 10.1017/S1461145709009948.
6. Katare YK, Piazza J E, Bhandari J, Daya R P, Akilan K, Simpson M J, Mishra, R K. Intranasal delivery of antipsychotic drugs. *Schizophr. Res*, 2017; 184: 2–13. doi:10.1016/j.schres.2016.11.027
7. Alagusundaram M, Chengaiah B, Gnanaprakas, K, Ramkanth, S, Madhusudhana C, Dhachinamoorthi C. Nasal drug delivery system an overview. *Int J Res Pharma Sci*, 2010; 1: 454-465.
8. Fortuna, A., Alves, G., Serralheiro, A., Sousa, J., & Falcão, A., Intranasal delivery of systemic-acting drugs: small-molecules and biomacromolecules, *Eur J Phar Biophar*, 2014; 88(1): 8-27. doi: 10.1016/j.ejpb.2014.03.004.
9. Tyler PC, Heather WG, Anumantha GK, Walter HH. Mechanism of intranasal drug delivery directly to the brain. *Life Sciences*, 2018; 195: 44-52. doi.org/10.1016/j.lfs.2017.12.025.
10. Rokade M, Tambe B and Ruparel M. *In Situ Gel -Sustained Nasal Drug Delivery*. *Int J Pharm Sci Res*, 2015; 6(12): 4958-66. doi: 10.13040/IJPSR.0975-8232.6(12).4958-66.
11. Marzouk MA, Osman DA, Abd El-Fattah AI. Formulation and in vitro evaluation of a thermoreversible mucoadhesive nasal gel of itopride hydrochloride. *Drug Dev Ind Pharm*, 2018; 44(11): 1857-1867. doi: 10.1080/03639045.2018.1504059.
12. Mathure D, Madan JR, Gujar KN, Tupsamundre A, Ranpise HA, Dua K. Formulation and Evaluation of Niosomal in situ Nasal Gel of a Serotonin Receptor Agonist, Buspirone Hydrochloride for the Brain Delivery via Intranasal Route. *Pharm Nanotechnol*, 2018; 6(1): 69-78. doi: 10.2174/2211738506666180130105919.
13. Belgamwar VS, Chauk D S, Mahajan HS, Jain SA, Gattani SG, Surana SJ. Formulation and evaluation of in situ gelling system of dimenhydrinate for nasal administration, *Pharm Dev and Tech*, 2009; 14(3): 240-248. doi: 10.1080/10837450802498910.

14. Leslie Citrome. Aripiprazole long-acting injectable formulations for schizophrenia: aripiprazole monohydrate and aripiprazole lauroxil, *Expert Rev. Clin. Pharmacol*, 2016; 9(2): 169-186. doi: 10.1586/17512433.2016.1121809 .
15. Uchida S, Hiraoka S, Namiki N. Development of gummi drugs of aripiprazole as hospital formulations. *Chem Pharm Bull (Tokyo)*, 2015; 63(5): 354-60. doi: 10.1248/cpb.c15-00038.
16. Nahata T, Saini TR. Formulation optimization of long-acting depot injection of Aripiprazole by using D-optimal mixture design. *PDA J Pharm Sci Techno*, 2009; 63(2): 113-122.
17. Trotta F, Zanetti M, Cavalli R. Cyclodextrin-based nanosponges as drug carriers. *Beilstein J Org Chem*, 2012; 8: 2091–2099. doi:10.3762/bjoc.8.235.
18. Cavalli R, Trotta F, Tumiatti W. Cyclodextrin-based Nanosponges for Drug Deliver. *Journal of Inclusion Phenomena and Macrocyclic Chemistry*, 2006; 56: 209–213. DOI 10.1007/s10847-006-9085-2.
19. Swaminathan S, Vavia PR, Trotta F, Cavalli R, Tumbiolo S, Bertinetti L, Coluccia S.. Structural evidence of differential forms of nanosponges of beta-cyclodextrin and its effect on solubilization of a model drug. *J Incl Phenom Macro*, 2012; 76(1-2): 201-211. doi:10.1007/s10847-012-0192-y.
20. Won C, Sahu A, Vilos C, Kamaly N, S-M, JH & Tae G. Bioinspired Heparin Nanosponge Prepared by Photo-crosslinking for Controlled Release of Growth Factors. *Scientific reports*, 2017; 7(1): 14351. <https://doi.org/10.1038/s41598-017-14040-5>.
21. Caldera F, Argenzian M, Trotta F, Dianzani C, Gigliotti L, Tannous M, Pastero L, Aquilano D, Nishimoto T, Higashiyama T, Cavalli R. Cyclic nigerosyl-1,6-nigerose-based nanosponges: An innovative pH and time-controlled nanocarrier for improving cancer treatment. *Carbohydr Polym*, 2018; 194: 111-121. doi: 10.1016/j.carbpol.2018.04.027.
22. Sherje AP, Dravyakar BR, Kadam D, Jadhav M. Cyclodextrin-based nanosponges: a critical review. *Carbohydr Polym*, 2017; 173: 37-49. doi: 10.1016/j.carbpol.2017.05.086.
23. Swaminathan S, Pastero L, Serpe L, Trotta F, Vavia P, Aquilano D, Trotta M, Zara G, Cavalli R. Cyclodextrin-based nanosponges encapsulating camptothecin: physicochemical characterization, stability and cytotoxicity. *Eur J Pharm Biopharm*, 2010; 74: 193–201. doi: 10.1016/j.ejpb.2009.11.003.

24. Sherafudeen SP, Vasantha PV. Development and evaluation of in situ nasal gel formulations of loratadine. *Res Pharm Sci*, 2015; 10: 466–476.
25. Yong CS, Choi JS, Rhee JD. Effect of sodium chloride on the gelation, gel strength and bioadhesive force of poloxamer gels. *Int J Pharm*, 2001; 275: 195-205. doi:10.1016/s0378-5173(01)00809-2.
26. Tas C, Ozcan Y, Savaser A, Baykara T. In Vitro and ex vivo permeation studies of chlorpheniramine maleate gels prepared by carbomer derivatives. *Drug dev Ind Pharm*, 2004; 30(6): 637-647. doi: 10.1081/ddc-120037665.
27. ICH Topic Q1 A (R2) Stability Testing of new Drug Substances and Products. International Conference on Harmonization of Technical requirements for Registration of Pharmaceuticals for Human Use, Geneva, Switzerland, 2005.
28. Yasir M, Sara UV. Solid lipid nanoparticles for nose to brain delivery of haloperidol: in vitro drug release and pharmacokinetics evaluation. *Acta pharmaceutica Sinica. B*, 2014; 4(6): 454-63. doi: 10.1016/j.apsb.2014.10.005.
29. Kulkarni JA, Avachat AM. Pharmacodynamic and pharmacokinetic investigation of cyclodextrin mediated asenapine maleate in situ nasal gel for improved bioavailability. *Drug Dev Ind Pharm*, 2017; 43(2): 234-245. doi: 10.1080/03639045.2016.1236808.
30. Recent advances in carrier mediated nose-to-brain delivery of pharmaceuticals Bourganis V, Olga Kammona, O Aleck Alexopoulos A, Costas Kiparissides C. *Eur J Pharm Biopharm*, 2018; 128: 337–362. <https://doi.org/10.1016/j.ejpb.2018.05.009>.